Third-order optical nonlinearity of gold nanoparticle arrays embedded in a $BaTiO_3$ matrix

Tingyin Ning,[1] Chunchong Chen,[2] Yueliang Zhou,[1,*] Heng Lu,[1] Hong Shen,[1] Dongxiang Zhang,[1] Pei Wang,[2] Hai Ming,[2] and Guozhen Yang[1,2]

[1]Beijing National Laboratory for Condensed Matter Physics, Institute of Physics, Chinese Academy of Sciences, Beijing 100190, China

[2]Anhui Key Laboratory of Optoelectronic Science and Technology, University of Science and Technology of China, Hefei, Anhui 230026, China

*Corresponding author: ylzhou@aphy.iphy.ac.cn

Received 29 September 2008; revised 10 December 2008; accepted 10 December 2008; posted 10 December 2008 (Doc. ID 102177); published 8 January 2009

$Au:BaTiO_3$ composite films comprising hexagon-shaped Au nanoparticle arrays covered with $BaTiO_3$ matrix were fabricated by double-layer nanosphere lithography and pulsed laser deposition technique. The optical nonlinearity of the composite film was determined using the Z-scan technique at a wavelength of 532 nm and a pulse duration of 25 ps. The third-order nonlinear optical susceptibility, $\chi^{(3)}$, was found to be 2.9×10^{-8} esu, which is comparable with the best values in metal–dielectric films comprising randomly distributed spherical particles but with much higher metal concentrations. The local electric field enhancement in and near the particles was investigated using the dipole discrete approximation method.

OCIS codes: 160.4330, 190.4720, 310.1860, 320.5390.

1. Introduction

Composite films consisting of nanosized metal particles embedded in dielectric matrices have attracted considerable interest due to their possible applications in nonlinear optical devices such as optical computing, switching, real time holography, and phase conjugators [1–3]. The greatly enhanced optical nonlinearities in these materials were well known to stem from the giant amplification of the local field near and inside the metal nanoparticles at the surface plasmon resonance (SPR). In recent years, various composite films doped with metal nanoparticles, such as $Au:TiO_2$ [4], $Ag:BaTiO_3$ [5], and $Cu:Al_2O_3$ [6], have been prepared using magnetron sputtering, laser ablating, solgel, ion implanting, and so on. Usually, the metal particles were spherical of various sizes and dispersed randomly in the dielectric matrices. Such composite films tend to show broad plasmon resonance owing to the inhomogeneous particle sizes and spatial distribution [1]. Recently, nanoparticle arrays of periodically arranged individual nanoparticles with the desired shape, size, and orientation have attracted much attention. Periodicity plays a key role in tuning the optical response of the ordered metal nanostructures and has been widely studied in experimental and theoretical investigations of plasmon-enhanced effects such as surface-enhanced Raman scattering, luminescence, extraordinary optical transmission, biological sensors, and optical nonlinearity [7–12].

Many well-established nanofabrication or microfabrication techniques were used to generate the periodic metal particle arrays, such as electron-beam lithography, which could produce nanostructures down to 10 nm with good reproducibility, and focused-ion-beam milling, which is used to prepare nanostructures, for example arrays of holes, on existing films. However, these techniques cost too much and have limitations on the sample size. Nanosphere lithography (NSL) as an inexpensive and

0003-6935/09/020375-05$15.00/0

high-throughput nanofabrication has been widely used to produce periodic nanostructures [13,14]. In this paper, we prepared Au nanoparticle arrays with Au arranged hexagonally in two-dimensional (2D) patterns on fused quartz substrates using double-layer nanosphere lithography (DSL). The nonlinear optical properties of composite film comprising Au nanoparticle arrays embedded in a $BaTiO_3$ matrix were investigated.

2. Experiment

Au nanoparticle arrays embedded in the $BaTiO_3$ matrix were fabricated using NSL and pulsed laser deposition (PLD). First, pure Au nanoparticle arrays were fabricated by NSL and a lift-off technique. A double-layer nanosphere crystal mask was formed by a self-assembly process. By dropping 10 μl of polystyrene nanospheres (with diameter $D = 200$ nm) diluted solution (0.5 wt.%) onto a clean quartz substrate, which was inclined about 3–5° in a chamber with saturated humidity at a temperature of about 30 °C, we successfully got a homogeneous, double-layer ordered nanosphere crystal mask. After the crystal mask was dry, it was mounted in a PLD chamber, and Au film was deposited onto the substrate through the interstices of polystyrene nanospheres. In a later lift-off process, the nanosphere mask was completely removed by ultrasonication in chloroform, and well-ordered Au nanoparticle arrays were obtained. Second, the substrate with Au nanoparticle arrays was mounted into the same PLD system, and the $BaTiO_3$ thin film was deposited onto the Au nanoparticles at a pressure of 1.0×10^{-3} Pa at 750 °C. Then, a composite film of nanoparticle arrays embedded in $BaTiO_3$ matrix was obtained successfully. The thickness of the $BaTiO_3$ layer is about 21 nm, according to a reference film of pure $BaTiO_3$ measured by a Dektak 8 surface stylus profiler (Veeco Company).

The nanostructures of the samples were investigated using atomic force microscopy (AFM, Nanoscope IIIa) in contact mode. The extinction spectra of the samples were measured from 200 to 800 nm using a spectrophotometer (SpectraPro-500i, Acton Research Corporation) at room temperature. The optical nonlinearities were determined by the single beam Z-scan technique, which has the advantage of separating the contributions of refractive and absorptive nonlinearities in the samples and giving the signs as well [15]. A mode-locked Nd:YAG laser at a wavelength of 532 nm and a pulse width of 25 ps was used as the light source. The laser beam was focused onto the sample by a 150 mm focal length lens with a pulse energy of 3.0 μJ at the focus. The beam waist was measured to be 30 μm, and the Rayleigh diffraction length was calculated to be 5.3 mm. The on-axis transmitted beam energy, the reference beam energy, and the ratios of them were measured using an energy ratiometer (EPM 2000, Coherent Inc.) simultaneously to remove the laser fluctuations. In order to reduce the possible thermal accumulative effect, the laser repetition rate was set to 1 Hz.

3. Results and Discussion

Figure 1(a) shows a 2D AFM image of a 5 μm × 5 μm area of pure Au nanoparticle arrays. Each particle should be hexagonal in shape according to the geometric analysis [14]. However, as evidenced in the AFM image, the particle shape was slightly smoothed during the NSL process. The interparticle spacing d of the periodic Au particles is given by $d = D$. The in-plane diameter, a_{DL}, defined as the distance of two parallel sides of the hexagon, is given by $a_{DL} = (\sqrt{3} - 1 - \frac{1}{\sqrt{3}})D = 0.155\,D$. In our experiment, the diameter of the nanosphere is $D = 200$ nm, so the interparticle spacing and the diameter of each Au nanoparticle are calculated to be 200 and 31 nm, respectively, which are in accord with the results of AFM measurement considering the tip-broadening effect. The value of diameter-spacing ratio $\gamma = d/a_{DL}$ is about 6.45. The out-of-plane height

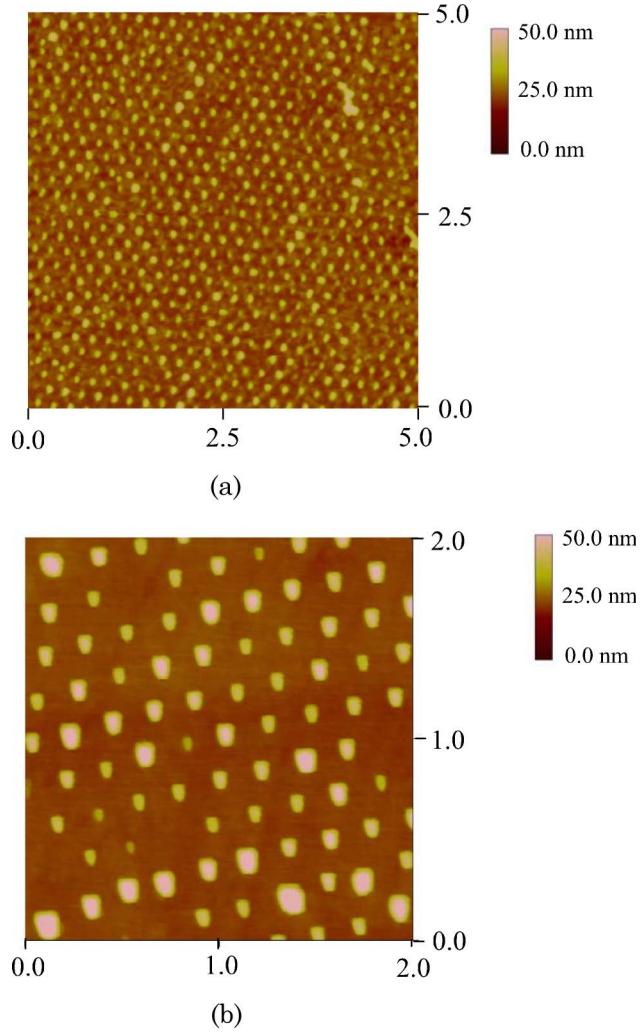

Fig. 1. (Color online) AFM images of (a) 5 μm × 5 μm area of pure Au nanoparticle arrays and (b) 2 μm × 2 μm area of Au:$BaTiO_3$ composite film.

of the nanoparticle arrays is about 15 nm, depending on the deposition time. Figure 1(b) shows a 2D AFM image of the composite film comprising Au nanoparticle arrays embedded in the $BaTiO_3$ matrix. The pattern of nanoparticle arrays could still be seen clearly because the $BaTiO_3$ film was very thin and it was deposited homogeneously both on the substrate and the top of Au nanoparticles. The volume fraction of Au nanoparticles was calculated to be about 1.7%.

The optical extinction spectra of the samples are shown in Fig. 2. As a reference, the optical extinction spectrum of $BaTiO_3$ thin film was also recorded, as shown in Fig. 2, curve (a). The absorption peak around 250 nm is attributed to $BaTiO_3$ thin film [16]. Figure 2, curve (b) shows the optical extinction spectrum of Au:$BaTiO_3$ composite film, and an obvious SPR peak near 625 nm was observed.

Figure 3 shows the typical open-aperture and closed-aperture Z-scan curves of the sample. The open circles indicate the measured data, with each point corresponding to the average value of ten pulses. The solid curve represents the theoretical fit [15]. As the fused quartz substrate has a very weak nonlinear optical response measured by the same Z-scan setup in our experiment, the observed large optical nonlinearities resulted from the composite film. The open-aperture curve shows a normalized transmittance peak, indicating the presence of nonlinear absorption saturation. The closed-aperture curve gives the valley–peak configuration, corresponding to a positive nonlinear refractive index.

The data were analyzed using the procedures described in Ref. [15]. The linear transmittance of the closed aperture, defined as the ratio of the pulse energy passing through the aperture to the total pulse energy, was measured to be 0.1. The value of ΔT_{p-v}, the difference between the normalized peak and the valley transmittance, can be obtained through the best theoretical fit of the Z-scan curve as shown in

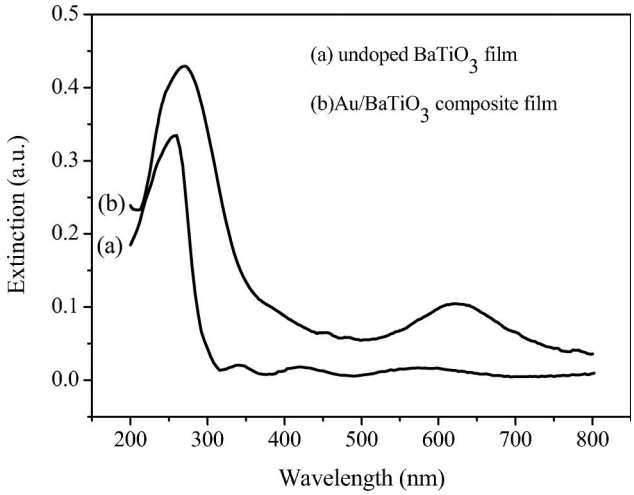

Fig. 2. Optical extinction spectra properties of Au nanoparticle arrays embedded in the $BaTiO_3$ matrix. The spectrum of undoped Au:$BaTiO_3$ film was also recorded as a reference.

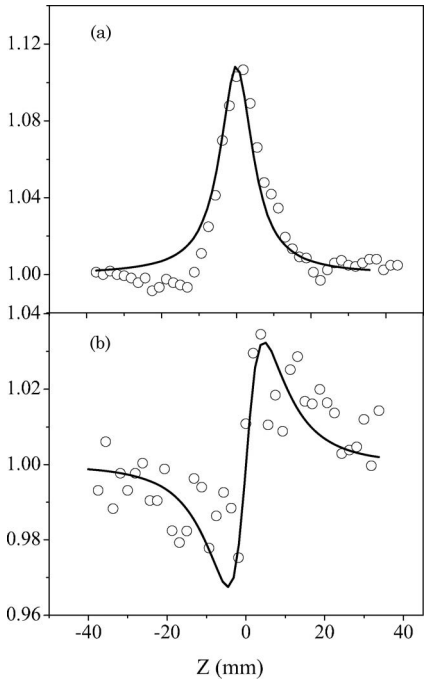

Fig. 3. (a) Open-aperture and (b) closed-aperture Z-scan curves of Au:$BaTiO_3$ composite film: circles, experimental data; curves, theoretical fit.

Fig. 3(b). The nonlinear refractive index, n_2, and the real part of the third-order nonlinear optical susceptibility, $\mathrm{Re}\chi^{(3)}$, of the sample were calculated to be $1.5 \times 10^{-14}\ m^2/W$ and 2.1×10^{-8} esu, respectively. The nonlinear absorption coefficient, β, and the imaginary part of the third-order nonlinear optical susceptibility, $\mathrm{Im}\chi^{(3)}$, were calculated to be 3.5×10^{-7} m/W and 2.0×10^{-8} esu, respectively. The absolute value of $\chi^{(3)}$ was obtained to be about 2.9×10^{-8} esu , which is comparable to the values of some representative metal/dielectric composite films with higher metal concentrations, such as Au:SiO_2 [17], Cu:Al_2O_3 [6], and Cu:$Ba_{0.5}Sr_{0.5}TiO_3$ [18].

The large optical nonlinearity of the composite film with such a low metal concentration could be attributed to the stronger local field of the gold metal nanoparticle arrays. Previous studies demonstrated that the nanoparticle arrays could narrow the SPR band compared with that in the composite films comprising randomly dispersed sphere-shaped Au particles with various sizes. The narrow bandwidth of the SPR extinction band in the spectral domain corresponds to a reduction of the damping of the plasmon oscillation, which leads to the enhanced local electric field [8,19]. Otherwise, the periodically arranged particles are of almost uniform size, so the scattered light fields in the plane of the particle arrays are of almost the same phase, producing a large local field [8]. Calculation results indicated that the intensity of the electromagnetic field of 2D nanoparticle arrays can be several orders of magnitude greater than that of a random metal–dielectric film at the percolation threshold [20]. Besides, the contributions of the nonspherical-shaped nanoparticle

should be considered. For composite films at low metal concentration, $\chi^{(3)}$ can be expressed by the following equation considering the third-order nonlinear optical susceptibility of metal itself, $\chi_m^{(3)}$ [21]:

$$\chi^{(3)} = pf^2|f|^2\chi_m^{(3)}, \tag{1}$$

where p is the volume fraction of metal particles embedded in composite film, $f = E_i/E_0$ is the local field factor (E_i is the local field, E_0 is the macroscopic field). f can be expressed as follows when the metal particles are spherical:

$$f = \frac{3\varepsilon_d}{\varepsilon_m + 2\varepsilon_d}, \tag{2}$$

where ε_d is the matrix dielectric permittivity and $\varepsilon_d = n_0^2$ for the $BaTiO_3$ matrix ($n_0 = 2.3$), ε_m is the metal–dielectric permittivity. In the large particle limit (>20 nm), it is appropriate to calculate the ε_m value from the bulk Au, and $\varepsilon_m = -4.64 + i2.41$ at the wavelength of 532 nm [22]. The value of $|f|^2$ was calculated to be about 6.13 according to Eq. (2). For metal particles with a nonspherical shape, Eq. (2) is invalid. The local field f will be a tensorial form because of the anisotropic-shaped particles and the polarized light. Dipole discrete approximation, which is a well-known method to solve the problem of light interaction with arbitrary-shaped particles [23], was used to calculate the local electric field near and inside the hexagon-shaped Au nanoparticles. The field wave vector, K, was perpendicular to the substrate, and the polarization of the electric field was assumed to be perpendicular to one side of Au nanoparticles. The local $|E_i|^2$ contours were plotted in Fig. 4, assuming $E_0 = 1$. It is clearly shown that the very intense contours are along the two sides of the hexagon-shaped Au particle. The value of $|f|^2$ is about 9 according to the calculation, which is about 1.5 times larger than that of the spheroidal particles. Meanwhile, the particles are of almost uniform size, so the local electric field of each particle has almost the same phase, which avoids the possibility of a cancellation effect between particles with different dielectric constant due to different sizes [24]. The anisotropic shape and uniform size of Au nanoparticles also contribute well to the enhancement of the optical nonlinearity.

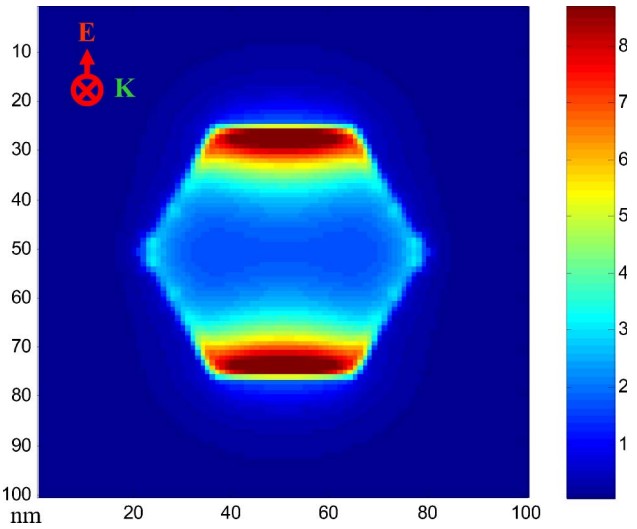

Fig. 4. (Color online) Local electric field enhancement ($|E|^2$) contours near the hexagonal Au nanoparticle embedded in the $BaTiO_3$ matrix at the wavelength of 532 nm, which is off the SPR.

4. Conclusions

In summary, a composite film comprising hexagon-shaped Au nanoparticles arrays embedded in $BaTiO_3$ matrix was fabricated by DSL and the PLD technique. The nonlinear optical properties of the sample were investigated by the Z-scan method at a wavelength of 532 nm with a pulse duration of 25 ps. The third-order nonlinear optical susceptibility was determined to be 2.9×10^{-8} esu, which is comparable with that of some random metal–dielectric films with higher metal concentrations. The local field enhancement contours near and inside the metal particles were investigated using discrete dipole approximation. The periodic arrangement and the anisotropy of Au nanoparticles contribute to the large local field enhancement.

The authors are grateful for the financial support of the National Natural Science Foundation of China, grant 10574157, and National Basic Research Program of China, 2006CB302900.

References

1. U. Kreibig and M. Vollmer, *Optical Properties of Metal Clusters*, Vol. 25 of Springer Series in Materials Science (Springer, 1995).
2. D. Ricard, P. Roussignol, and C. Flytzanis, "Surface-mediated enhancement of optical phase conjugation in metal colloids," Opt. Lett. **10**, 511–513 (1985)
3. S. A. Maier and H. A. Atwater, "Plasmonics: localization and guiding of electromagnetic energy in metal/dielectric structures," J. Appl. Phys. **98**, 011101 (2005).
4. H. B. Liao, R. F. Xiao, H. Wang, K. S. Wong, and G. K. L. Wong, "Large third-order optical nonlinearity in Au:TiO_2 composite films measured on a femtosecond time scale," Appl. Phys. Lett. **72**, 1817–1819 (1998).
5. G. Yang, W. T. Wang, Y. L. Zhou, H. B. Lu, G. Z. Yang, and Z. H. Chen, "Linear and nonlinear optical properties of Ag nanocluster/$BaTiO_3$ composite films," Appl. Phys. Lett. **81**, 3969–3971 (2002).
6. J. M. Ballesteros, R. Serna, J. Solis, C. N. Afonso, A. K. Petford-Long, D. H. Osborne, and R. F. Haglund, Jr., "Pulsed laser deposition of Cu:Al2O3 nanocrystal thin films with high third-order optical susceptibility," Appl. Phys. Lett. **71**, 2445–2447 (1997).
7. M. Meier, A. Wokaun, and P. F. Liao, "Enhanced fields on rough surfaces: dipolar interactions among particles of sizes exceeding the Rayleigh limit," J. Opt. Soc. Am. B **2**, 931–949 (1985).
8. B. Lamprecht, G. Schider, R. T. Lechner, H. Ditlbacher, J. R. Krenn, A. Leitner, and F. R. Aussenegg, "Metal nanoparticle gratings: influence of dipolar particle interation on the plasmon resonance," Phys. Rev. Lett. **84**, 4721–4274 (2000).

9. L. Baia, M. Baia, J. Popp, and S. Astilean, "Gold films deposited over regular arrays of polystyrene nanospheres as highly effective SERS substrates from visible to NIR," J. Phys. Chem. B **110**, 23982–23986 (2006).
10. A. J. Haes, S. Zou, G. C. Schatz, and R. P. Van Duyne, "Nanoscale optical biosensor: short range distance dependence of the localized surface plasmon resonance of noble metal nanoparticles," J. Phys. Chem. B **108**, 6961–6968 (2004).
11. H. Shen, G. Lu, M. Ou, C. A. Marquette, G. Ledoux, S. Roux, O. Tillement, P. Perriat, B. Chen, and Z. Chen, "How the morphology of biochips roughness increases surface-enhanced chemiluminescence," Chem. Phys. Lett. **439**, 105–109 (2007).
12. H. Shen, B. Chen, G. Lu, T. Ning, D. Guan, Y. Zhou, and Z. Chen, "Enhancement of optical nonlinearity in periodic gold nanoparticle arrays," Nanotechnology **17**, 4274–4277 (2006).
13. H. W. Deckman and J. H. Dunsmuir, "Natural lithography," Appl. Phys. Lett. **41**, 377–379 (1982).
14. J. C. Hulteen and R. P. Van Duyne, "Nanosphere lithography: A materials general fabrication process for periodic particle array surfaces," J. Vac. Sci. Technol. A **13**, 1553–1558 (1995).
15. M. Sheik-Bahae, A. A. Said, T. H. Wei, D. J. Hagan, and W. Van Stryland, "Sensitive measurement of optical nonlinearities using a single beam," IEEE J. Quantum Electron. **26**, 760–769 (1990).
16. H. Z. Guo, L. F. Liu, Z. H. Chen, S. Ding, H. B. Lu, K.-J. Jin, Y. L. Zhou, and B. L. Cheng, "Structure and optical properties of $BaTiO_3$ ultrathin films," Europhys. Lett. **73**, 110–115 (2006).
17. M. Y. Lee, T. S. Kim, and Y. S. Choi, "Third-order optical nonlinearities of solgel-processed Au-SiO2 thin films in the surface plasmon absorption region," J. Non-Cryst. Solids **211**, 143–149 (1997).
18. J. S. Kim, K. S. Lee, and S. S. Kim, "Third-order optical nonlinearity of Cu nanoparticle-dispersed $Ba_{0.5}Sr_{0.5}TiO_3$ films prepared by alternating pulsed laser deposition," Thin Solid Films **515**, 2332–2336 (2006).
19. S. Zou and G. C. Schatz, "Silver nanoparticle array structures that produce giant enhancements in electromagnetic fields," Chem. Phys. Lett. **403**, 62–67 (2005).
20. D. A. Genov, A. K. Sarychev, V. M. Shalaev, and A. Wei, "Resonant field enhancements from metal nanoparticle arrays," Nano Lett. **4**, 153–158 (2004).
21. I. Tanahashi, Y. Manabe, T. Tohda, S. Sasaki, and A. Nakamura, "Optical nonlinearities of Au/SiO_2 composite thin films prepared by a sputtering method," J. Appl. Phys. **79**, 1244–1249 (1996).
22. P. B. Johnson and R. W. Christy, "Optical constants of the noble metals," Phys. Rev. B **6**, 4370–4379 (1972).
23. E. M. Purcell and C. R. Pennypacker, "Scattering and adsorption of light by nonspherical dielectric grains," Astrophys. J. **186**, 705–714 (1973).
24. D. D. Smith, G. Fischer, R. W. Boyd, and D. A. Gregory, "Cancellation of photoinduced absorption in metal nanoparticle composites through a counterintuitive consequence of local field effects," J. Opt. Soc. Am. B **14**, 1625–1631 (1997).